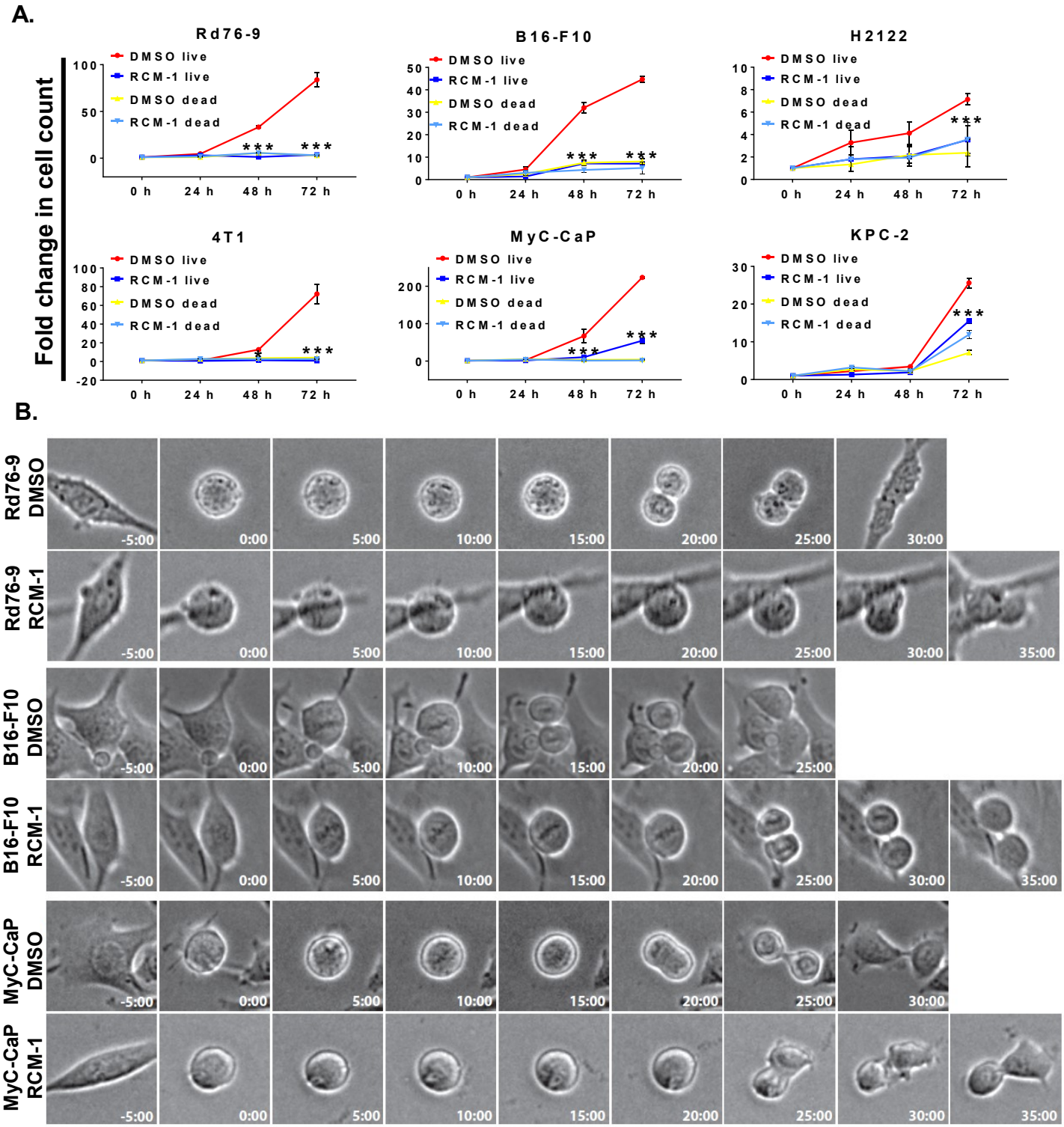

Supplemental Figure S1. RCM-1 inhibits cell proliferation and reduces mitotic index. (A) RCM-1 inhibits cellular proliferation of Rd76-, B16-F10, H2122, 4T1, MyC-CaP and KPC-2 cells in culture. Cell growth was analyzed by counting live and dead cells stained with trypan blue. Cells treated with DMSO were used as controls. Graphs show fold change in the number of cells compared to 0 h time point. Graphs represent data from three independent experiments. mean±SD. *$p < 0.05$, **$p < 0.01$ and ***$p < 0.001$ compared to DMSO-treated control. **(B)** Time-course depiction of mitotic divisions after RCM-1 treatment in B16-F10, MyC-CaP and Rd76-9 cells. Live images of tumor cells were acquired on an epifluorescence microscope. 4 fields per well were imaged every 5 min for 2-3 days, using a 20x LD objective. Representative frames of time-lapse movies of mitotic Rd76-9, B16-F10 and MyC-CaP cancer cells treated with DMSO (control) and RCM-1. Scale bar, 20 µm. Time, min:sec. Supplemental movies (see attached files). Images were acquired by spinning-disk confocal microscopy.

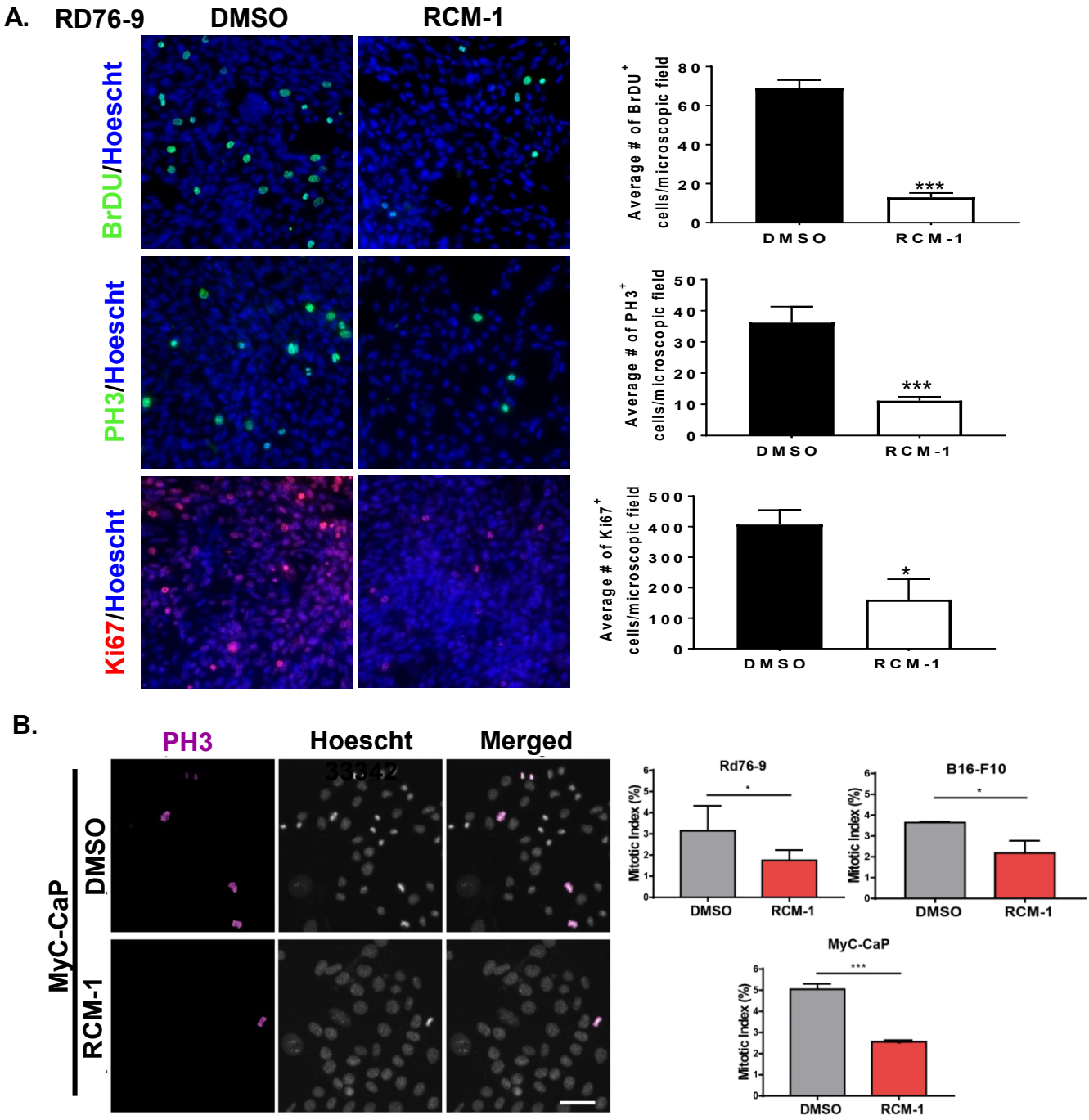

Supplemental Figure S2. RCM-1 inhibits mitosis and DNA replication. **(A)** Rd76-9 tumor cells were incubated with BrdU, and subsequently fixed and stained with anti-BrdU antibody. Cells were also stained for PH3 and Ki67 following fixation. Panel on the left shows representative fields of BrdU (green, upper panel)-, PH3 (green, middle panel)-, Ki67 (Red, lower panel)- positive Rd76-9 cells in the DMSO and RCM-1-treated groups after 48 h (magnification x400). Graphs represent the average number of DMSO- and RCM-1-treated tumor cells positive for BrdU, PH3 and Ki67 (10 microscopic fields per sample, magnification x200). **(B)** RCM-1 decreases the mitotic index. Rd76-9, B16-F10 and MyC-CaP tumor cells were stained for mitotic marker phospho-serine 10-Histone 3 (PH3). Panel on the left shows representative fields of DMSO- and RCM-1-treated MyC-CaP cells (PH3 staining, magenta; DNA staining, grey). Graphs represent the percentage of DMSO- and RCM-1-treated tumor cells staining positive for PH3 (n>1000 cells per condition). *$p < 0.05$, **$p < 0.01$ and ***$p < 0.001$ and ****$p \leq 0.0001$ by Fisher's exact statistical test.

Shukla et al. Supplemental Figure S3

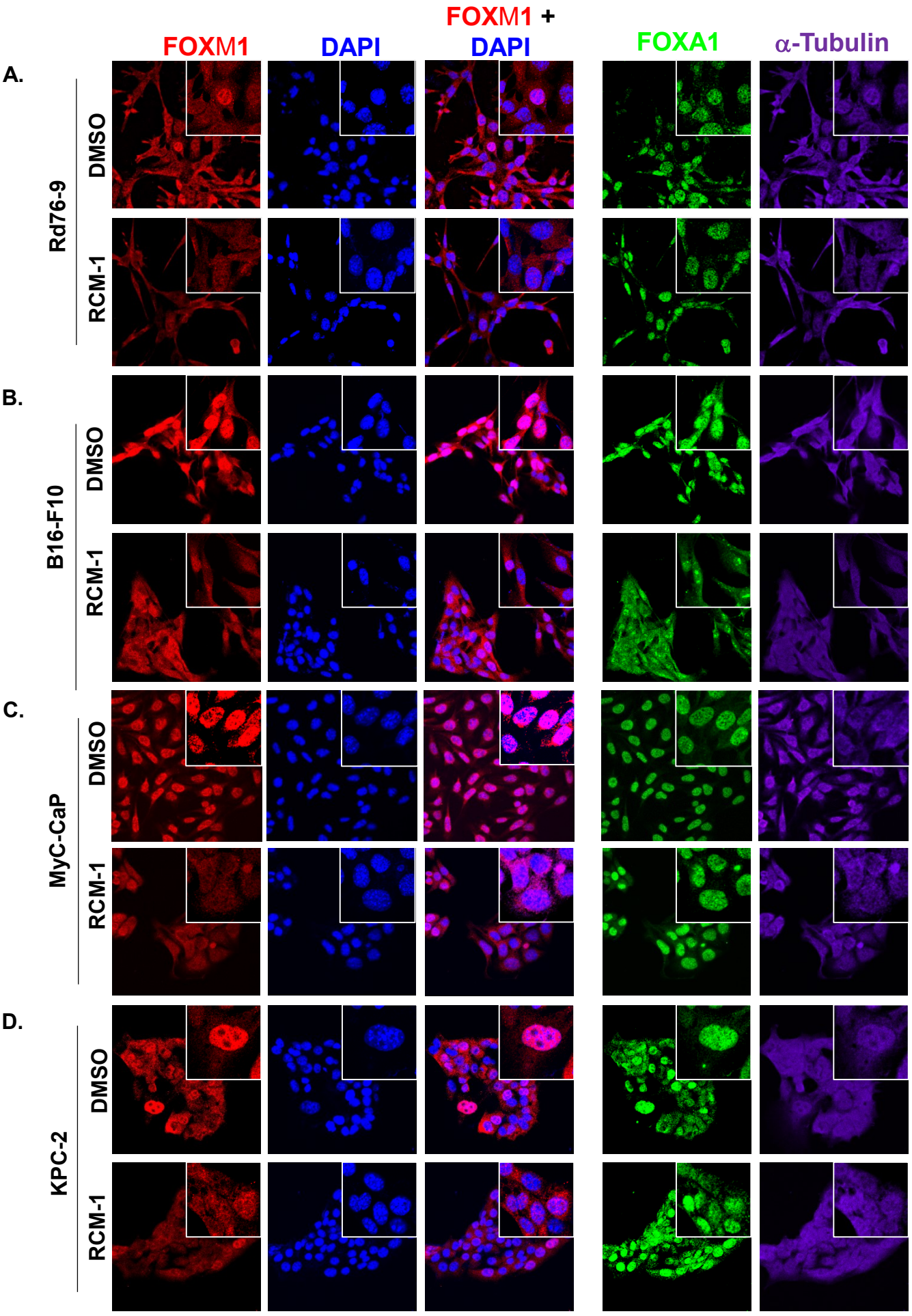

Supplemental Figure S3. RCM-1 decreases the expression and nuclear localization of FOXM1 *in vitro*. **(A)** Rd76-9, **(B)** B16-F10, **(C)** MyC-CaP and **(D)** KPC-2 tumor cells were treated with DMSO or RCM-1 for 24 h and subsequently fixed and stained for FOXM1-AF594 (red), FOXA1-AF488 (green) and α-

Supplemental Figure S2. RCM-1 inhibits cell proliferation and increases duration of mitotic division and cell cycle. Time-course depiction of mitotic divisions after RCM-1 treatment in B16-F10, MyC-CaP and Rd76-9 cells. Live images of tumor cells were acquired on an epifluorescence microscope. 4 fields per well were imaged every 5 min for 2-3 days, using a 20xLD objective. Representative frames of time-lapse movies of mitotic Rd76-9, B16-F10 and MyC-CaP cancer cells treated with DMSO (control) and RCM-1. Scale bar, 20 μm. Time, min:sec. Supplemental movies (see attached files). Representative videos showing mitotic divisions of control (DMSO) and RCM-1 treated tumor cells. Images were acquired by spinning-disk confocal microscopy. tubulin (cyan) followed by confocal imaging. DAPI (blue) was used to visualize cell nuclei. Images are representative of 6 random microscopic fields in each treatment group (magnification x600).

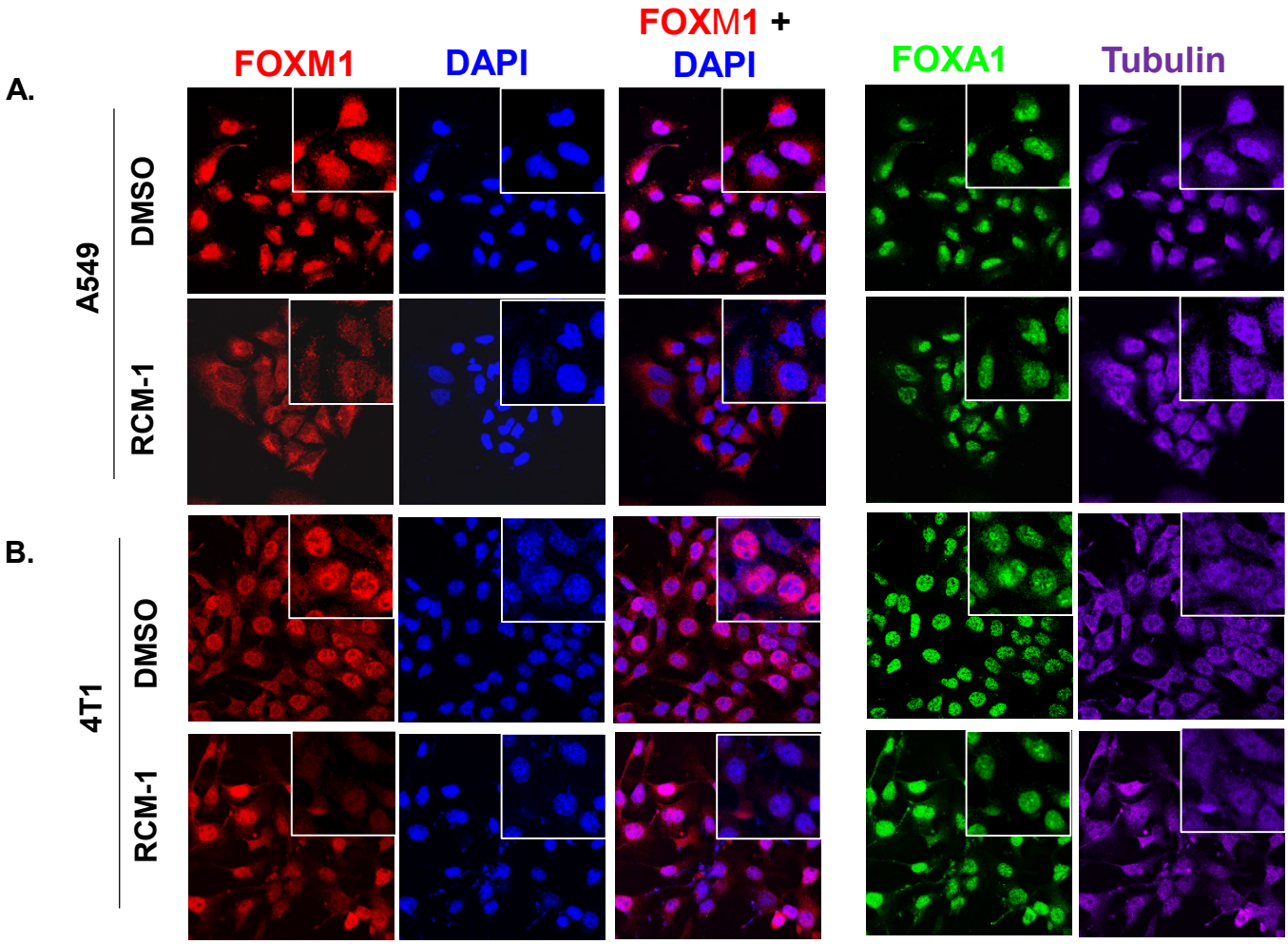

Supplemental Figure S4. RCM-1 decreases expression and nuclear localization of FOXM1. (A) A549 and **(B)** 4T1 cells were treated with either DMSO or RCM-1 for 24 h and then stained for FOXM1-AF594 (red), FOXA1-AF488 (green) and α-tubulin (cyan) followed by confocal imaging. DAPI (blue) was used to visualize cell nuclei. RCM-1 decreased nuclear localization of FOXM1 but did not affect FOXA1 localization. Images are representative of 5 random microscopic fields in each treatment group (magnification x600).

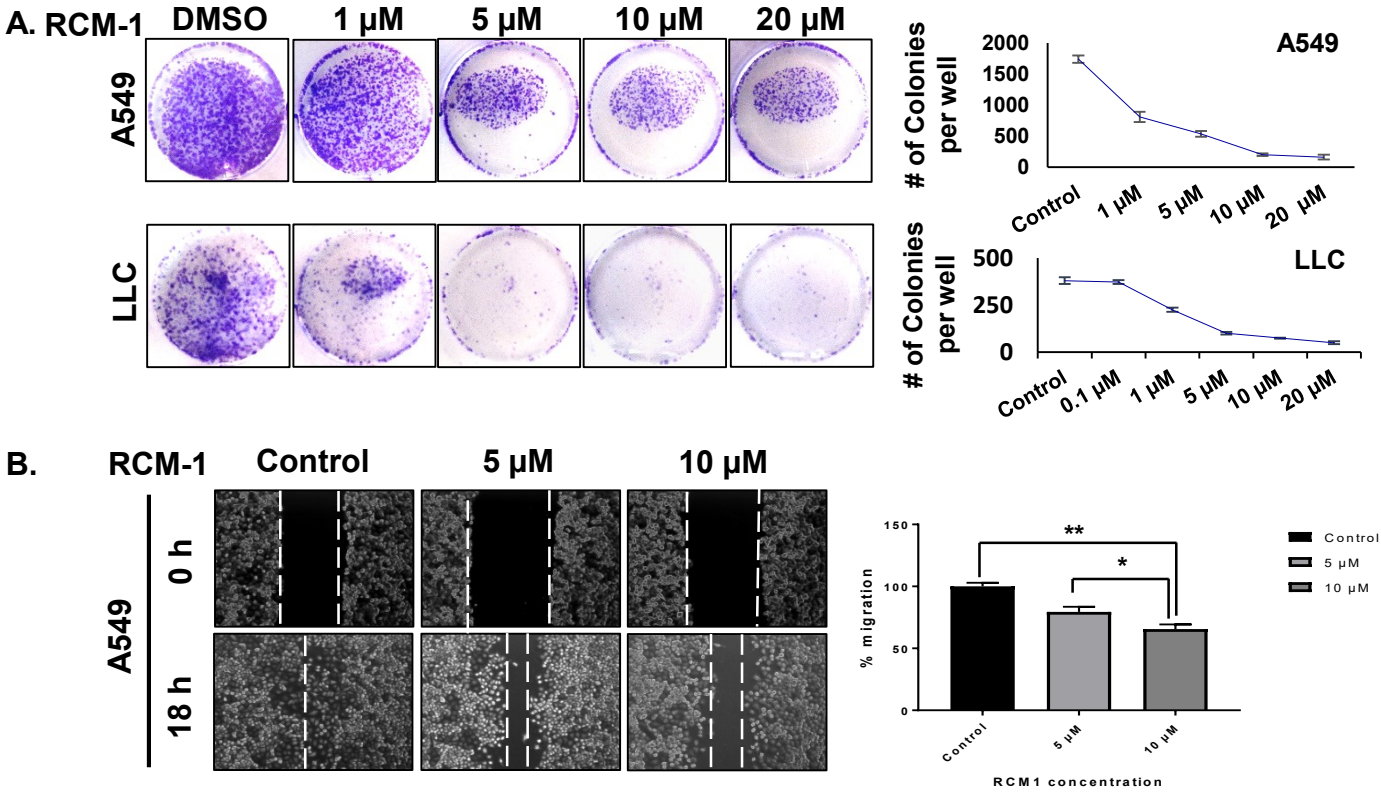

Supplemental Figure S5. RCM-1 decreases clonogenicity and migration of tumor cells *in vitro*. (A) Human A549 and mouse LLC lung tumor cells were treated with RCM-1. DMSO-treated cells were used as controls. At day 7, colonies were fixed and stained with 0.5% crystal violet and average numbers of DMSO- or RCM-1-treated colonies containing ≥50 cells were counted. Results were obtained from three independent experiments. Graphs represent average number of tumor cell colonies in different treatment groups (mean±SE). **(B)** Standardized scratches were created in subconfluent A549 cells. Cells were treated with RCM-1 and cell migration was assessed after 18 h. Data were presented as percent migration in RCM-1-treated groups compared to DMSO treatment (mean±SE). *$p < 0.05$, **$p < 0.01$ and ***$p < 0.001$ compared to DMSO-treated control.

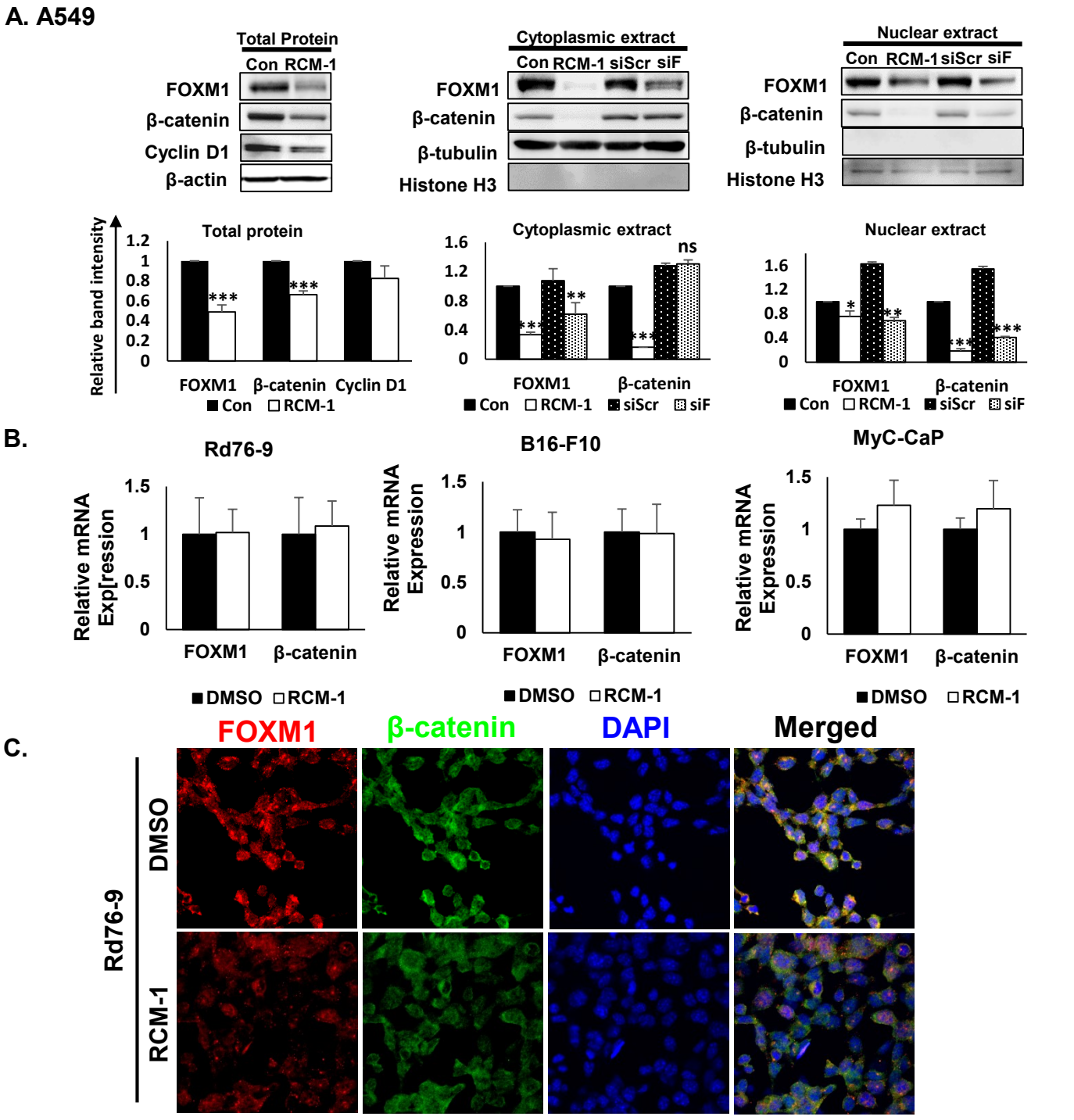

Supplemental Figure S6. RCM-1 inhibits FOXM1 and β-catenin levels and nuclear localization (A) Whole cell lysates, cytoplasmic and nuclear extracts of RCM-1-treated and siFOXM1-transfected- A549 cells were analyzed for expression of FOXM1, β-catenin and Cyclin D1. DMSO-treated or shScrambled-transfected cells were used as controls. β-actin, α/β-tubulin, and Histone H3 were used as loading controls for whole cell lysates, cytoplasmic-, and nuclear extracts, respectively. Blots are representative of three independent experiments. Graphs represent relative band intensities (mean±SE). *$p < 0.05$, **$p < 0.01$ and ***$p < 0.001$ compared to DMSO-treated control. **(B)** RCM-1-treated Rd76-9, B16-F10, MyC-CaP, KPC-2 and A549 tumor cells were analyzed for mRNA expression of FOXM1 and β-catenin. DMSO-treated cells were used as controls. β-actin was used as control. Graphs represent relative mRNA expressions in different treatment groups (mean±SE). *$p < 0.05$, **$p < 0.01$ and ***$p < 0.001$ compared to DMSO-treated control. **(C)** Rd76-9 cells were treated with DMSO or RCM-1 for 24 h and cells were then fixed and stained for FOXM1 (red) and β-catenin (green) followed by confocal imaging. DAPI (blue) was used visualize cell nuclei. RCM-1 decreased expression and nuclear localization of FOXM1 and β-catenin. Images are representative of 5 random microscopic fields in each treatment group (magnification x600).

Shukla et al. Supplemental Figure S7

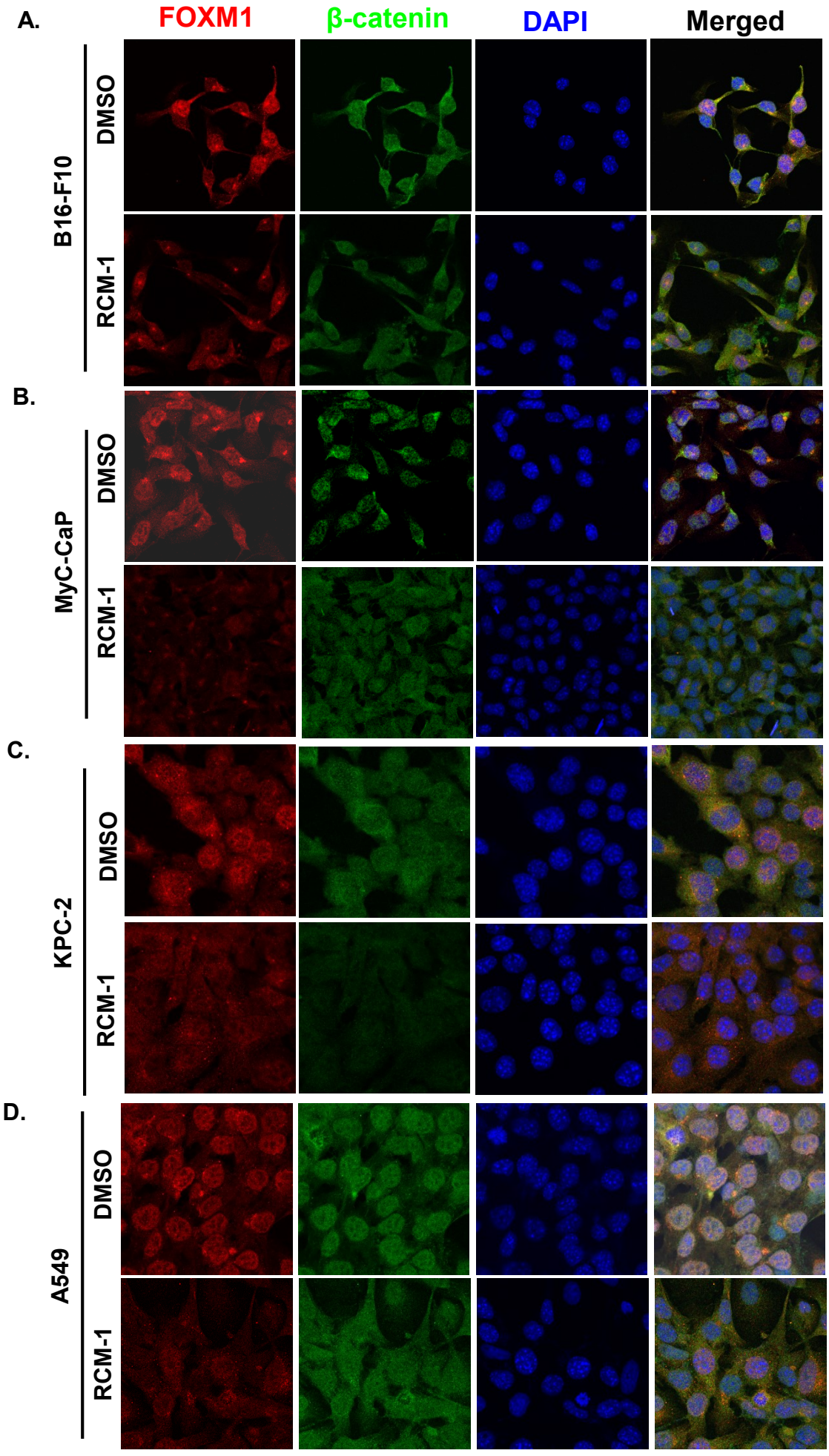

Supplemental Figure S7. RCM-1 decreased expression and nuclear localization of FOXM1. (A) B16-F10, **(B)** MyC-CaP **(C)** KPC-2, and **(D)** A549 cells were treated with either DMSO or RCM-1 for 24 h and stained for FOXM1-AF594 (red), FOXA1-AF488 (green) and α-tubulin (cyan) followed by confocal imaging. DAPI (blue) was used to visualize cell nuclei. RCM-1 decreased nuclear localization of FOXM1 but did not affect FOXA1 localization. Images are representative of 5 random microscopic fields in each treatment group (magnification x600).

Shukla et al. Supplemental Figure S8

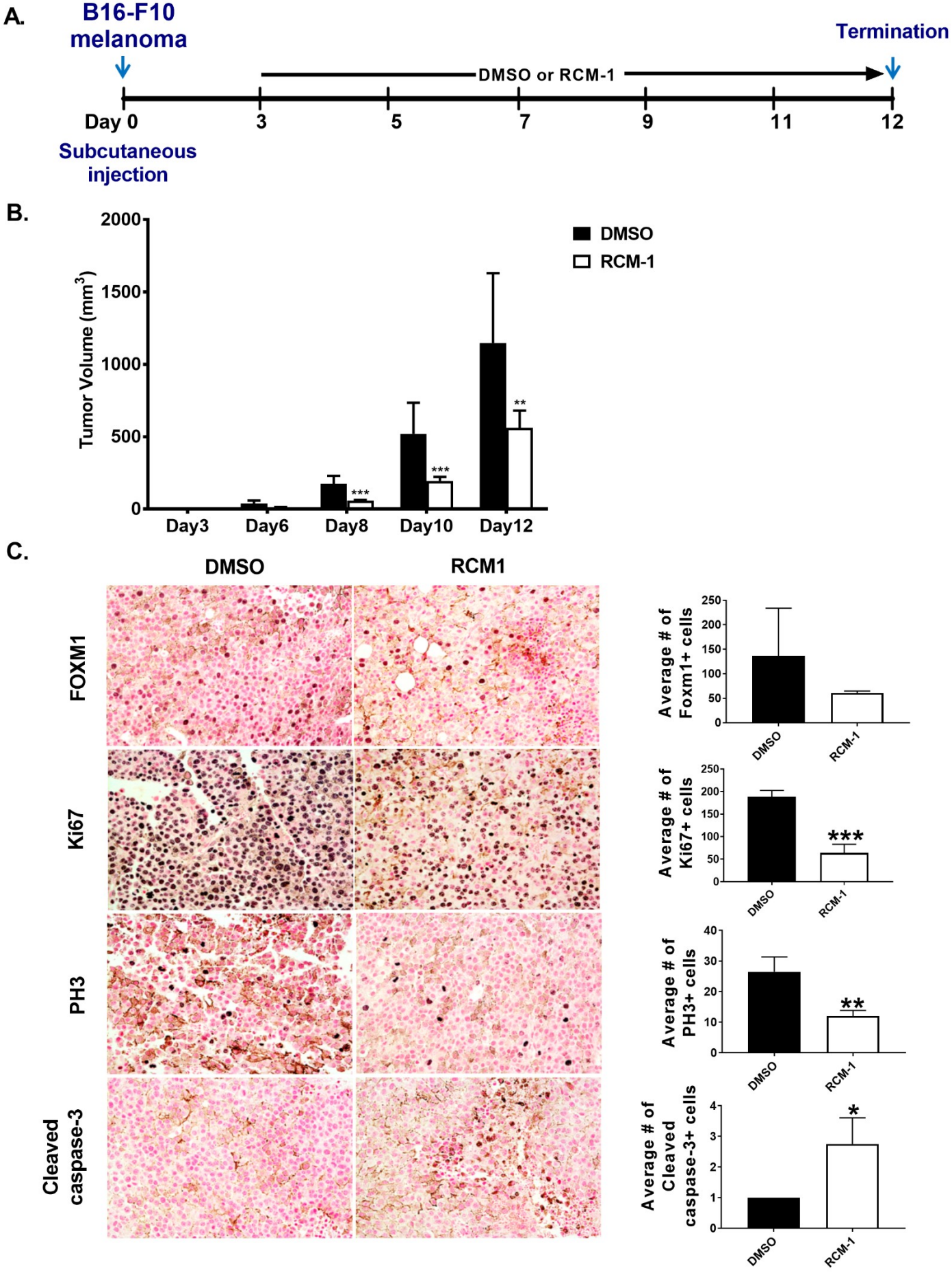

Supplemental Figure S8. RCM-1 treatment reduces growth of B16-F10 melanoma tumors in mice. (A) Schematic representation of experimental protocol. B16-F10 cells were injected subcutaneously into C56Bl/6J mice (n=7). Three days after tumor cell inoculation, animals were injected with vehicle (DMSO) or RCM1 (20 mg/Kg b.w.) every other day. On day 12, animals were sacrificed, and tumors were harvested. **(B)** RCM-1 decreased B16-F10 orthotopic tumor growth. Graph shows average tumor volume per group (mean±SD). **(C)** RCM-1 treatment decreased tumor cell proliferation and increased apoptosis in B16-F10 melanoma tumors. Paraffin-embedded sections of B16-F10 tumors were stained with antibodies against FOXM1, Ki67, PH3 and cleaved caspase-3 and photographed (magnification x200). RCM-1-treated B16-F10 tumors showed significantly reduced immunolabeling of proliferation markers Ki67 and PH3. Staining for cleaved caspase-3 was increased in RCM-1-treated tumors. Graphs in right panel show average numbers of FOXM1-, Ki67-, PH3- and cleaved caspase-3-positive cells. Positive cells (dark brown) were counted in 5 random microscopic fields per group and numbers are presented as mean±SD. $*p < 0.05$, $**p < 0.01$ and $***p < 0.001$ compared to the DMSO-treated control group.

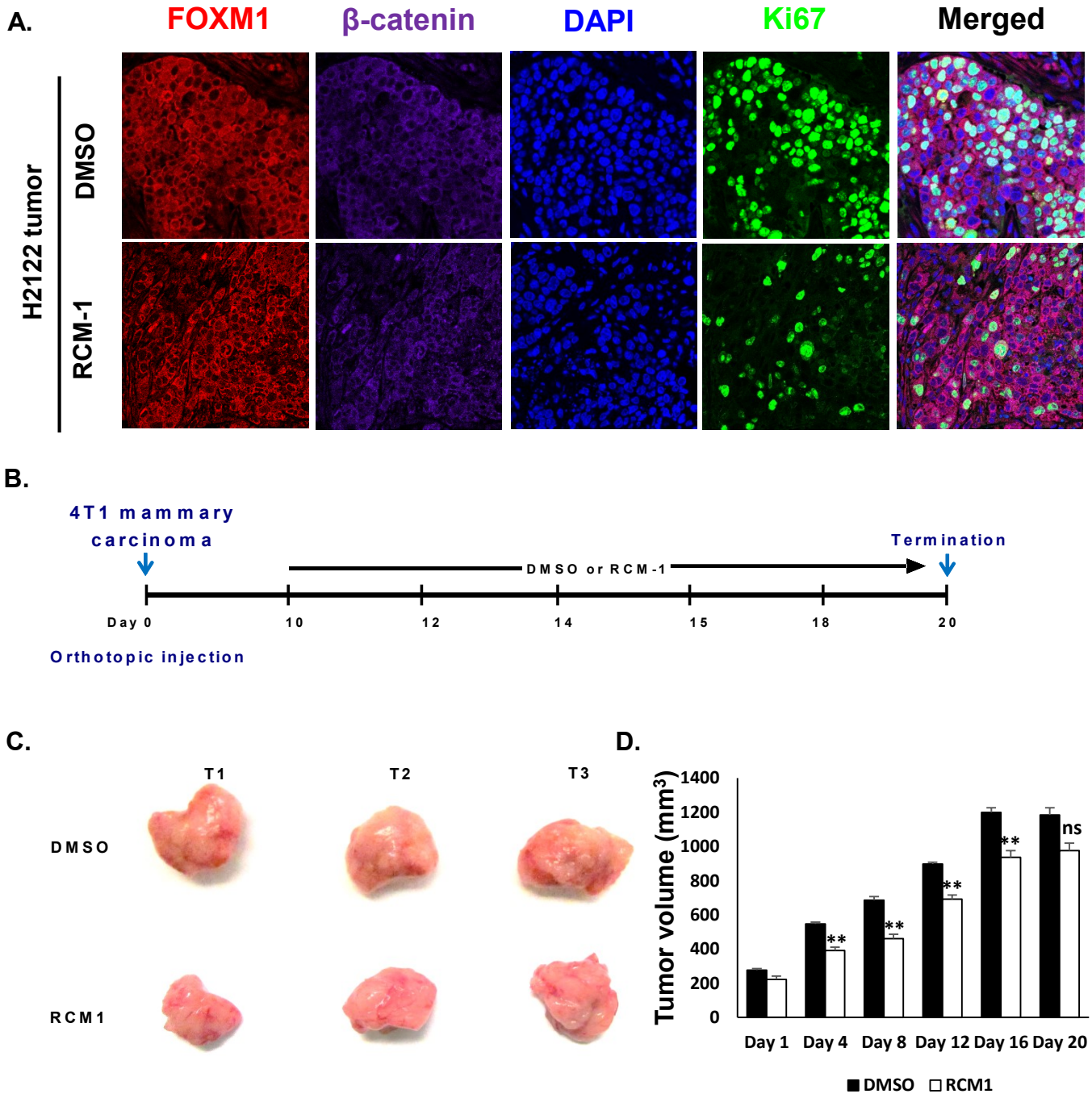

Supplemental Figure S9. Effect of RCM-1 on H2122 and 4T1 carcinogenesis (A) RCM-1 decreased FOXM1 and β-catenin immunostaining in H2122 tumors. Immunofluorescence analysis of paraffin-embedded sections of DMSO- or RCM-1-treated tumors with antibodies against FOXM1 and β-catenin showed a reduction in immunostaining in the RCM-1-treated group compared to DMSO-treated tumors (magnification x600). Images are representative of 5 random microscopic fields per group. **(B)** Balb/C mice were inoculated with 4T1 breast adenocarcinoma tumor cells and treated with RCM-1 for 20 days (every other day starting at day 10 after inoculation of tumor cells). DMSO-treated mice were used as controls. **(C)** Representative image shows tumor sizes of DMSO- or RCM-1-treated mice. **(D)** Graph represents tumor volumes of DMSO- or RCM-1-treated groups. mean±SD. *$p < 0.05$, **$p < 0.01$ and ***$p < 0.001$ compared to the DMSO-treated control group.

A. **Mass chromatogram of mouse serum 30 min after intraperitoneal administration of RCM-1**

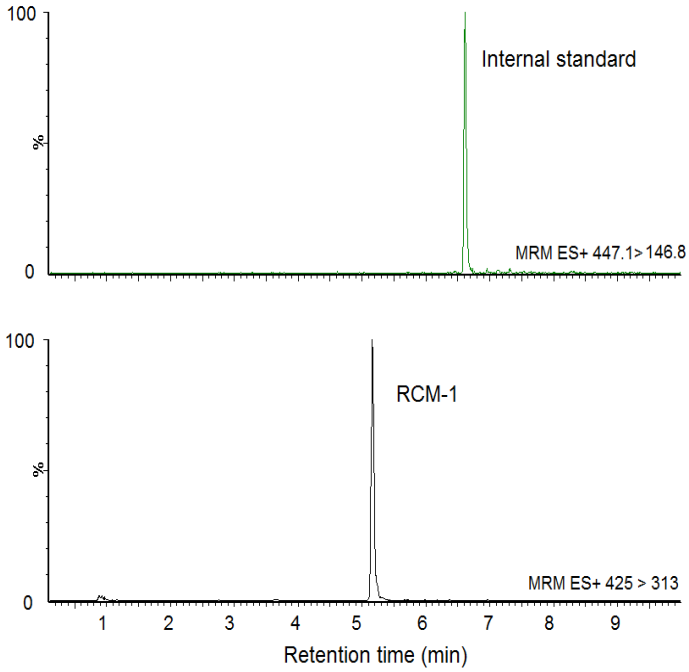

B. **Mass spectra of RCM-1 and internal standard**

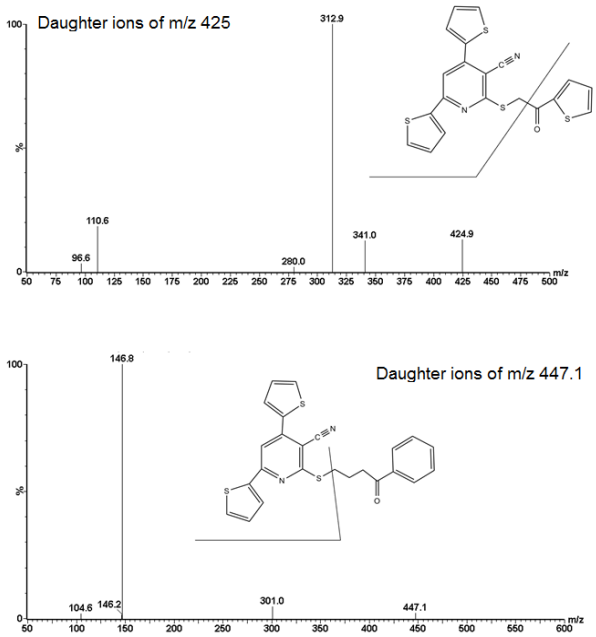

C.

Time	RCM-1 concentration (ng/mL)	SD
Baseline	1	0
15 min	5161	4487
30 min	5603	8050
1 h	5895	5187
2 h	7064	2702
5 h	2540	837
10 h	936	779
24 h	159	93

D.

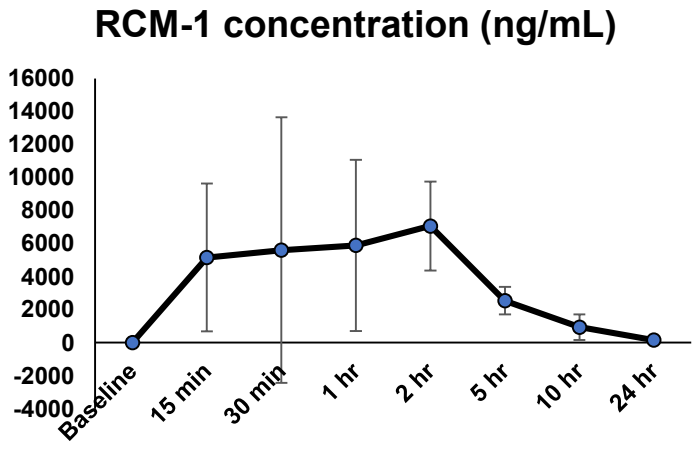

Supplemental Figure S10. UPLC-MS analysis of RCM-1 concentrations in serum. (A-B) The method used for analysis of RCM-1 identifies clear peak for RCM-1 compared with internal standard, depicting successful method development for compound identification. **(C-D)** C56Bl/6J mice (n=3 per group) were treated with a single dose of 20 mg/Kg b.w. RCM-1 and serum was collected at indicated intervals. RCM-1 concentrations in serum were analyzed by UPLC-MS analysis. Table and graph depict average RCM-1 concentrations (ng/mL) at each time point per group.

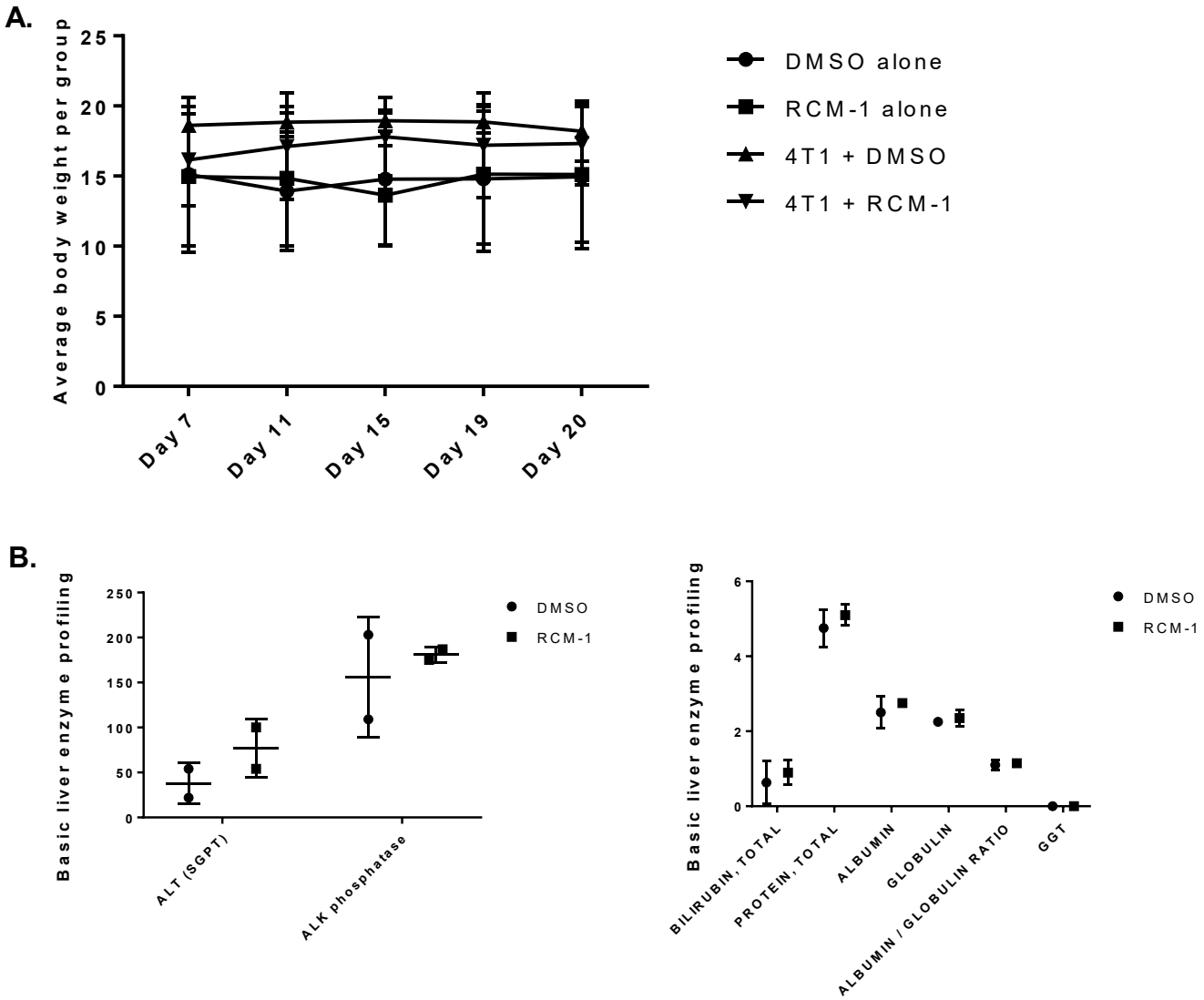

Supplemental Figure S11. RCM-1 treatment does not alter body weight or liver enzyme profiles. (A) Graph shows average body weight of different groups of mice. **(B)** Graphs show effect of RCM-1 treatment on different liver enzymes in serum. Serum from DMSO-treated animals was used as control.

Supplemental Table T1. Serum RCM-1 concentrations

Time points	RCM-1 concentration (ng/mL)
Mouse Serum Baseline #1	ND
Mouse Serum Baseline #2	1
Mouse Serum Baseline #3	0
Mouse Serum 15 min #1	8986
Mouse Serum 15 min #2	6274
Mouse Serum 15 min #3	222
Mouse Serum 30 min #1	734
Mouse Serum 30 min #2	14895
Mouse Serum 30 min #3	1180
Mouse Serum 1 h #1	3051
Mouse Serum 1 h #2	2753
Mouse Serum 1 h #3	11882
Mouse Serum 2 h #1	8626
Mouse Serum 2 h #2	3943
Mouse Serum 2 h #3	8621
Mouse Serum 5 h #1	3501
Mouse Serum 5 h #2	1972
Mouse Serum 5 h #3	2147
Mouse Serum 10 h #1	1563
Mouse Serum 10 h #2	1182
Mouse Serum 10 h #3	64
Mouse Serum 24 h #1	215
Mouse Serum 24 h #2	211
Mouse Serum 24 h #3	52

Supplemental movie 1. Live imaging to measure the cell cycle and mitotic duration in Vehicle-treated Rd76-9 cells. Live images of control Rd76-9 cells were acquired on an epifluorescence microscope by spinning-disk confocal microscopy. 4 fields per well were imaged every 5 min for 2-3 days, using a 20x LD objective.

Supplemental movie 2. Live imaging to measure the cell cycle and mitotic duration in RCM-1-treated Rd76-9 cells. Live images of RCM-1-treated Rd76-9 cells were acquired on an epifluorescence microscope by spinning-disk confocal microscopy. 4 fields per well were imaged every 5 min for 2-3 days, using a 20x LD objective.

Supplemental movie 3. Live imaging to measure the cell cycle and mitotic duration in Vehicle-treated B16-F10 cells. Live images of control B16-F10 cells were acquired on an epifluorescence microscope by spinning-disk confocal microscopy. 4 fields per well were imaged every 5 min for 2-3 days, using a 20x LD objective.

Supplemental movie 4. Live imaging to measure the cell cycle and mitotic duration in RCM-1-treated B16-F10 cells. Live images of RCM-1-treated B16-F10 cells were acquired on an epifluorescence microscope by spinning-disk confocal microscopy. 4 fields per well were imaged every 5 min for 2-3 days, using a 20x LD objective.

Supplemental movie 5. Live imaging to measure the cell cycle and mitotic duration in Vehicle-treated MyC-CaP cells. Live images of control MyC-CaP cells were acquired on an epifluorescence microscope by spinning-disk confocal microscopy. 4 fields per well were imaged every 5 min for 2-3 days, using a 20x LD objective.

Supplemental movie 6. Live imaging to measure the cell cycle and mitotic duration in RCM-1-treated MyC-CaP cells. Live images of RCM-1-treated MyC-CaP cells were acquired on an epifluorescence microscope by spinning-disk confocal microscopy. 4 fields per well were imaged every 5 min for 2-3 days, using a 20x LD objective.